ARTICLE

Simulation of the Electromechanical Behavior of Multiwall Carbon Nanotubes

A. Pantano[†,*] and M. Buongiorno Nardelli[‡,§,*]

[†]Dipartimento di Meccanica, Università degli Studi di Palermo, Viale delle Scienze, 90128 Palermo, Italy, [‡]Center for High Performance Simulation and Department Physics, North Carolina State University, Raleigh, North Carolina 27695, and [§]CCS-CSM, Oak Ridge National Laboratory, Oak Ridge, Tennessee 37831-6359

ABSTRACT The enormous potential of carbon nanotubes (CNTs) as primary components in electronic devices and NEMS necessitates the understanding and predicting of the effects of mechanical deformation on electron transport in CNTs. In principle, detailed atomic/electronic calculations can provide both the deformed configuration and the resulting electrical transport behavior of the CNT. However, the computational expense of these simulations limits the size of the CNTs that can be studied with this technique, and a direct analysis of CNTs of the dimension used in nanoelectronic devices seems prohibitive at the present. Here a computationally effective mixed finite element (FE)/tight-binding (TB) approach able to simulate the electromechanical behavior of CNT devices is presented. The TB code is carefully designed to realize orders-of-magnitude reduction in computational time in calculating deformation-induced changes in electrical transport properties of the nanotubes. The FE-TB computational approach is validated in a simulation of laboratory experiments on a multiwall CNT and then used to demonstrate the role of the multiwall structure in providing robustness to conductivity in the event of imposed mechanical deformations.

KEYWORDS: carbon nanotubes · mechanical deformation · electron transport · finite element · tight-binding

The effects of mechanical deformation on the electron transport behavior of carbon nanotubes (CNTs) are of primary interest due to the enormous potential of nanotubes in making electronic devices and nanoelectromechanical systems (NEMS). Moreover, the ability of accurately predicting the effects of mechanical deformation on electron transport in CNTs could lead to quantitative evaluation of defects of actually synthesized CNTs since the role of imperfections, like missing atoms, could be fully understood and used in evaluating the CNTs that have been produced. Significant changes in CNT conductivity are linked to structural features, including diameter, chirality, and distortions,[1,2] giving behavior ranging from narrow-gap or moderate-gap semiconducting to metallic. Conduction in defect-free CNTs has been observed to be ballistic in nature, implying the absence of inelastic scattering and involving little energy dissipation.[3] Progress in theoretical understanding as well as experimental study and device realization in this field has been rapid;[3−19] already several prototypical devices have been constructed and demonstrated.[20] Most discussions of the electronic structure of CNTs assume perfect cylindrical symmetry, but this is somewhat of an oversimplification. High-resolution images of CNTs often disclose structural deformations such as bent, twisted, or collapsed tubes. Numerical simulations of the electromechanical behavior of CNTs mostly focus on SWNTs rather than on the more abundant MWNTs, and the few studies available in the literature deal with small segments of only two- or three-walled CNTs.[16−19] This is mainly due to the high computational burden involved in atomistic (*i.e.*, *ab initio*, tight-binding, molecular dynamics) simulation of MWNTs of realistic dimensions. An alternative approach can be based on analytical techniques as in the works of Pugno *et al.*,[21−23] where an analytical model based on the energy method in both small deformation and finite kinematics regimes is used to interpret electromechanical measurements on MWNTs. However, analytical models usually require simplifying assumptions in the geometry or other aspects of the problem limiting their range of use. This holds true also for the work of Pugno *et al.*,[21−23] where a cylindrical shape for the MWNTs is assumed; this simplification exposes the analytical model to possible reduction in its accuracy if the walls of the MWNTs are affected by buckling. In order to enable and optimize CNTs as a basic building block of a new nanoelectronic technology, a sufficient understanding of both the electrical and mechanical proper-

*Address correspondence to apantano@dima.unipa.it, mbnardelli@ncsu.edu.

Received for review July 13, 2009 and accepted September 14, 2009.

Published online September 22, 2009. 10.1021/nn900795n CCC: $40.75

ties, as well as their dependence on mechanical deformations, must be achieved.

Here we present a mixed finite-element tight-binding approach able to simulate the electromechanical behavior of SWNTs and MWNTs of the dimensions used in nanoelectronic devices. To realize the extreme computational savings necessary to work with realistically sized CNTs, first a continuum-level representation of nanotubes has been developed. Individual tubes are modeled using shell finite elements, where a specific pairing of elastic properties and mechanical thickness of the tube wall enables successful modeling with elastic shell theory. Using quadrilateral shell elements, it is possible to create a FE mesh of a CNT wall in which the FE nodal coordinates correspond to the atomic positions. Successive 60° rotations of shell element pairs bisecting a hexagonal cell in three superimposed FE meshes cancel the artificial mechanical anisotropy caused by any single-orientation quadrilateral meshing of the cell. The effects of nonbonded forces generated from the attractive and repulsive forces, due, respectively, to van der Waals and to Pauli's exclusion principles, are simulated with special interaction elements that are of critical importance in tube/tube or tube/substrate interactions, as well as in maintaining the interwall separation in deformed MWNTs. This new nonlinear structural mechanics-based approach for modeling CNTs has been verified by comparisons with MD simulations and high-resolution micrographs available in the literature; for details on the current mechanical implementation, the reader is referred to our previous works.[24−27]

Within the FE program simulating the mechanical deformation of the nanotube structure, the evolving atomic [nodal] coordinates are further processed using a tight-binding (TB) code which calculates deformation-induced changes in electrical transport properties of the nanotube. There the coordinates are used in TB calculations to compute electronic properties of the system. Our main objective is to predict effects of deformation on the electrical properties of MWNTs; hence, adopting a conventional TB code would negate the computational savings obtained by using the structural mechanics approach to compute the deformed atomic coordinates. Instead, an innovative TB algorithm was developed that results in substantial computational savings. Beginning with a recently developed approach, the coherent transport properties of infinitely long or finite conductors spanning the distance between two leads can be computed using two different full sp^3, four-orbital, orthogonal TB models[28a,b] or a nonorthogonal TB model.[28c] For details on the quantum conductance calculations, the reader is referred to our previous work.[13] Here, the full sp^3, four-orbital, orthogonal TB model model[28c] has been used. Then starting from the methodology for computing the conductance of a system with a large number of atoms presented in our previous work,[29] a novel approach has been developed where each CNT is divided along its length into a given number of shorter CNT segments connected to one another at interfaces. The system is equivalent to the original CNT, but the memory requirements and the computational expenses are reduced by orders of magnitudes. The realized computational efficiencies increase with increasing dimensions of the nanotube; for example, the analysis of a (70,70) tube had a memory requirement almost 5 orders of magnitude smaller than a conventional coding implementation of the TB algorithm. The portion of the (70,70) tube that is allowed to deform was divided along its length in 207 pieces since the matrices on which the program operates are square with dimensions

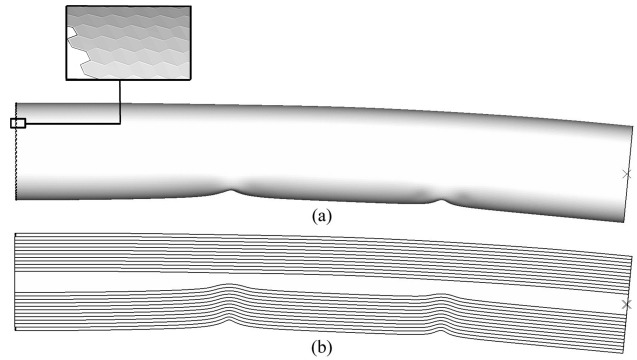

Figure 1. Final deformed configuration of the FE model reproducing the experiment, shown both in (a) a side view of the entire MWNT and (b) a diametral sectional view.

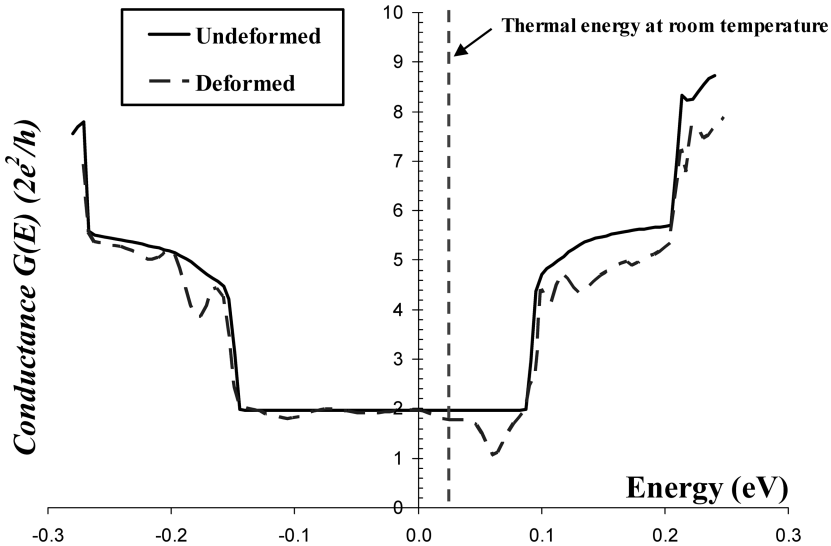

Figure 2. Conductance calculated using the mixed FE-TB approach for the model reproducing the MWNT used in the experiment, both in the undeformed and deformed configurations. The thermal energy at room temperature is also indicated.

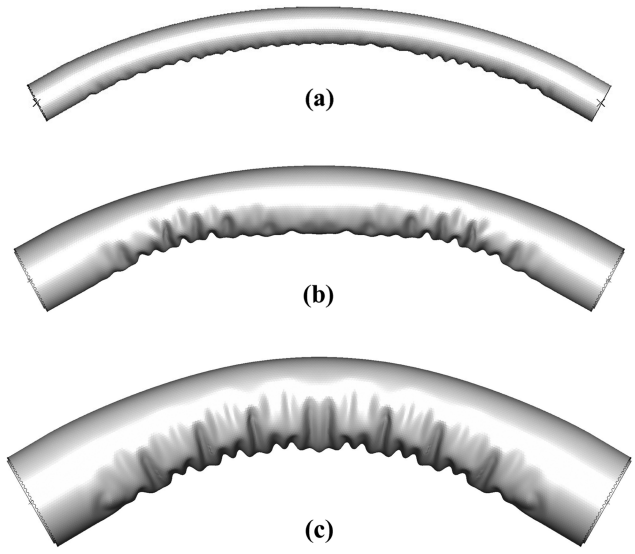

Figure 3. Sectional views of the final deformed configurations of the FE models producing the same bending angle of 60° in (a) the (30,30), (b) the (50,50), and (c) the (70,70) MWNTs.

equal to (number of atoms) × (number of orbitals per atom),[2] the reduction in the memory requirement is equal to 207 × 207 = 42 849.

RESULTS AND DISCUSSION

Here we utilize our electro-mechanical modeling technique to reproduce the MWNT laboratory experiments of Kuzumaki and Mitsuda,[30] who evaluated deformation-induced changes in electrical conductivity of a multiwall carbon nanotube. They measured electrical conductance during the deformation of MWNTs in a transmission electron microscope (TEM). Using a nanoprobe manipulation unit consisting of a fixed stage and a piezo-driven stage fitted into a TEM holder, they applied a compressive axial load on a MWNT, along with a bias voltage between the two stages. A combination of axial compression and bending deformation observable in the TEM was induced in the CNT. For more details about the experimental setup and the testing methodology, the reader is referred to Kuzumaki *et al.*[30] The applied bias voltage between tips was fixed at 1 V, while the current through the MWNT was measured during deformation, starting from the undeformed configuration. In the undeformed configuration, the current measured through the nanotube exceeded 115 μA under an applied bias voltage of 1 V; the resistance of the MWNT obtained is $R = V/I = 8696$ Ω. This value is not far from the resistance of an ideal metallic nanotube, 6450 Ω, indicating that the contact resistance is limited and not predominant as in other experiments available in literature. Since the undeformed conductance is near the theoretical one, we take the outermost CNT to be an armchair metallic (70,70) nanotube in the FE-TB model. Kuzumaki and Mitsuda[30] recorded a 10−12% reduction in the conductance when the MWNT was deformed to the level shown in their image.[30] As the authors noted, the MWNT was not damaged (*e.g.*, no Stone−Wales transition) at the imposed deformation level: the local radius of curvature at the deepest kink of the two buckling units formed was not small enough to cause a complete and irreversible sp^2 to sp^3 transition.[31,32] This was confirmed by measurements after loading was removed: the nanotube recovered its original undeformed shape, and the current returned to its initial level.

As previously motivated, the outermost wall is assumed to be an armchair CNT, thus showing metallic behavior. The model is 60 nm long, and the diameter of the outermost tube is 9.492 nm. It is compressed and bent by fixing the atoms of each wall near the two ends, and then displacing these 4 nm long rigid portions; thus, the deformable part of the model is 52 nm long. Figure 1 shows the FE model in its deformed configuration, both a side view of the outer surface and a diametral sectional view, with an inset illustrating the hexagonal meshing of the tube. The model reproducing the MWNT used in the experiment was gradually deformed by imposing a combination of axial compression and bending loading until the same configuration as in the TEM image[30] was reached.

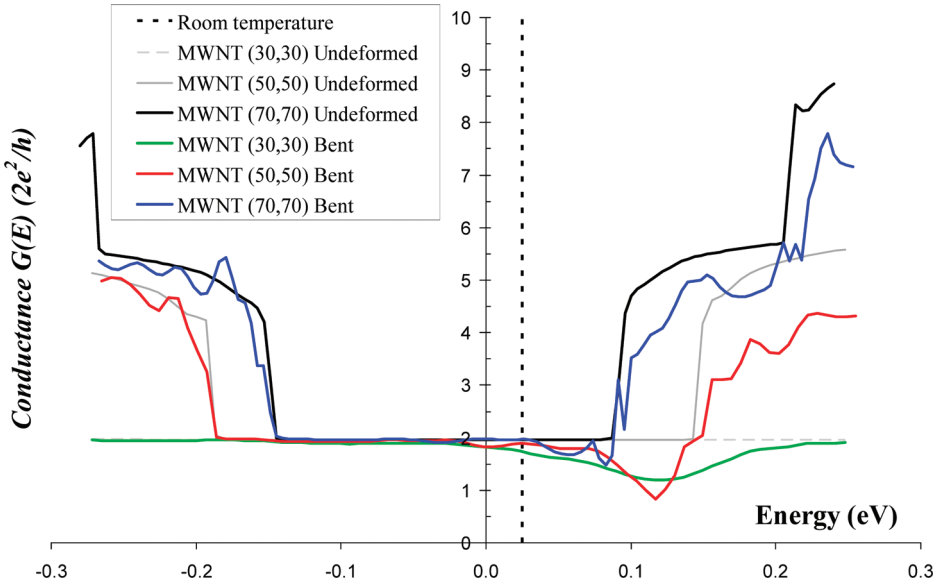

Figure 4. Conductance calculated using the mixed FE-TB approach for three armchair MWNT models of different outer diameters, both in the undeformed and deformed configurations.

Atomic coordinates, in both the undeformed and

TABLE 1. Comparison of the Undistorted Circumferential Lengths of the Three MWNTs Both in Value and as Percentage with Respect to the Total Circumference of Each Tube

MWNT	circumference of each tube	length of the circumference unaffected by the wrinkling	percentage of circumference unaffected by the wrinkling with respect to the total circumference
(30,30) MWNT	12.82 nm	9.35 nm	73%
(50,50) MWNT	21.3 nm	15.33 nm	72%
(70,70) MWNT	29.82 nm	20.95 nm	70%

deformed configurations, were passed to the TB code for computing the transport properties of the MWNT. For a bias voltage of 1 V, the overall conductance of the undeformed tube obtained from the mixed FE-TB approach was the theoretical one, $G = 2G_0$. At room temperature, the thermal energy kT is about 0.025 eV. Once the deformation level reached that shown in Figure 1, the TB code predicted about a 12% reduction in room-temperature conductance. These results are shown in Figure 2 as a plot of conductance *versus* energy, where the Fermi energy is taken as a reference and shifted to zero. On the basis of a computed conductance change similar to that reported in the experiments, the accuracy of the current predictions is considered to be rather good. A quick calculation can show that the temperature in the room where the experiment has been performed could have varied by a lot without effect on the 12% reduction in conductance measured in the experiment for the MWNT in the deformed configuration. The thermal energy kT was taken to be 0.025 eV because the Boltzmann constant $k = 8.617 \times 10^{-5}$ eV/K, and the temperature was assumed to be $T = 293$ K; in this case, $kT = (8.617 \times 10^{-5}) \times 293 = 0.025$ eV. According to the numerical results in Figure 2, if we increase or reduce the temperature by 20 K, the value of the conductance would remain the same: kT(at 273 K) $= (8.617 \times 10^{-5}) \times 273 = 0.0235$ eV and kT(at 313 K) $= (8.617 \times 10^{-5}) \times 293 = 0.0269$ eV. The temperature could grow up to 500 K before the conductance of the MWNT in the deformed configuration undergoes a further reduction: kT(at 500 K) $= (8.617 \times 10^{-5}) \times 500 = 0.043$ eV.

With this validation of the computational approach, we now investigate the effect of MWNT outer diameter on the mechanical deformation dependence of conductance. In addition to the (70,70) MWNT described above, models of (50,50) and (30,30) armchair MWNTs were created and subjected to bending loading conditions. The new undeformed models resemble the (70,70) tube shown in Figure 1; the only differences consisted of removing the outer two walls of the (70,70) to produce the 6.78 nm outer-diameter (50,50) mesh, and the outer four walls for the 4.08 nm outer-diameter (30,30) mesh. The three nanotubes were bent by fixing the atoms of each wall near the two ends, as done in the previous simulation of the (70,70) MWNT, and then gradually rotating these rigid portions of the tube. A bending angle of $\theta = 1.0472$ radians (60°) is gradually applied, imposing global curvature $\kappa = \theta/L$; the final κ is 0.0214 (1/nm) since the deformable part of the model is 52 nm long. The deformed configurations are shown in Figure 3a−c.

For a bias voltage of 1 V, the computed overall conductance of all three undeformed tubes was the theoretical value, $G = 2G_0$. Once the deformation levels reached those shown in Figure 3, the TB code predicted a reduction in conductance that varied over the considered energy range of −0.3 to 0.3 eV. Figure 4 plots conductance *versus* energy for all three MWNTs, and the Fermi energy is again taken as a reference and shifted to zero. At the same curvature, the conductance of MWNTs depends on the outer diameter. At room temperature, the smaller the outer diameter the greater

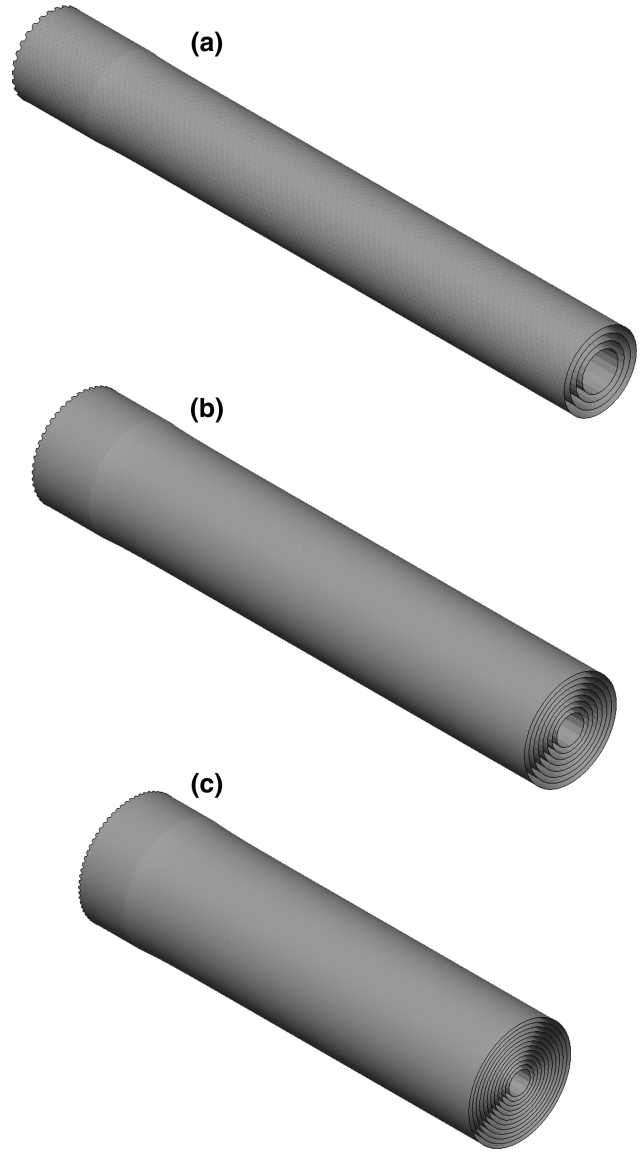

Figure 5. Views of the final 3D deformed configurations of the FE models in (a) the (30,30), (b) the (50,50), and (c) the (70,70) MWNTs. The figure shows only half of the carbon nanotube models.

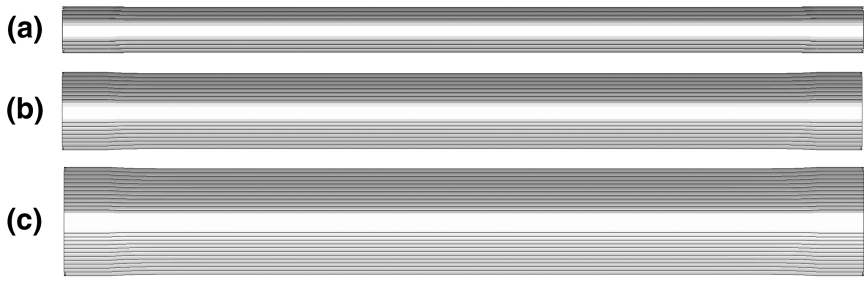

Figure 6. Sectional views of the final deformed configurations of the FE models in (a) the (30,30), (b) the (50,50), and (c) the (70,70) MWNTs.

the average drop in the conductance: the (30,30), (50,50), and (70,70) shows, respectively, a 13, 5.5, and 0% reduction in the conductance. It also can be noticed that the range of energy values where the conductance is reduced from the initial undeformed value, $G = 2G_0$, is larger for the smaller diameter MWNTs.

On the basis of the outcomes of these simulations, we identified the length of the circumference unaffected by the wrinkling as one of the possible geometrical features of the deformed configuration able to determine the dependence of conductivity on the MWNT diameter. In Table 1, the undistorted circumferential lengths of the three MWNTs are compared both in value and as percentage with respect to the total circumference of each tube. Even if the percentages are about the same, there is a big difference in the value of the lengths of the circumference unaffected by the wrinkling. In the (70,70) MWNT, the undistorted circumferential length is 2.24 times longer than that in the (30,30) and 1.366 longer than that in the (50,50).

In MWNTs, the nested van der Waals interactions of the increased number of inner walls radially stiffen the tube, thus limiting the circumferential extent of the kink. The number of relatively undistorted atoms outside the kinked portion of the circumference grows with the outer diameter. In the areas of the nanotube walls where a kink is present, due to the distortion caused by the bending, centers of scattering are created that reduce the conductivity. At any kink, the local bonding structure is deformed and the electrons will lose some of the π character of their corresponding orbitals. As stated in ref 32, the curvature in the nanotube walls due to the kink leads to a loss of spatial overlap of the atomic p orbitals that contribute to conjugation and a shift in hybridization of the atoms from the sp^2 of graphite to something intermediate between sp^2 and sp^3. The net result of these orbital effects is an increase in energy locally and an introduction of partial radical character in the π-bonding electrons. Smaller nanotubes have a smaller undistorted circumferential length (smaller number of atoms in position to provide an effective transport pathway) than the larger diameter MWNTs, thus giving the corresponding larger influence on the loss in conductivity.

Here we investigate one of the possible effects of MWNT outer diameter on the dependence of conductance on mechanical deformation. Models of (70,70), (50,50), and (30,30) armchair MWNTs were created and subjected to traction loading conditions. All of the models are 60 nm long, while the diameter of the outermost tube of the (70,70), (50,50), and (30,30) armchair MWNTs are, respectively, 9.492, 6.78, and 4.08 nm. The three nanotubes were stretched out by fixing the atoms of each wall near the two ends, then displacing these 4 nm long rigid portions of the tubes. An extension of 2.55 nm was gradually applied, imposing global axial deformation of 0.0472, since the deformable part of the model is 52 nm long. The deformed configurations are shown in Figures 5 and 6. Clearly, these are not pure tension boundary conditions, but an attempt to reproduce a possible real working condition for MWNT-based electronic devices where the ends of the nanotubes are fixed inside metallic leads and cannot deform. Near the fixed ends, there is a quick variation in the diameters of the deformed MWNTs clearly visible in Figures 5 and 6. In the areas of the nanotube walls where a curva-

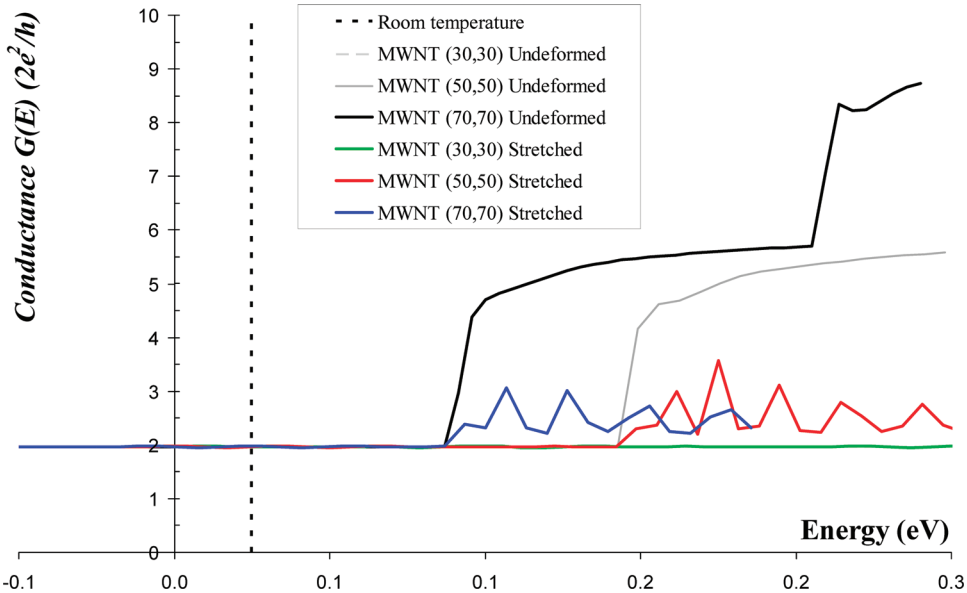

Figure 7. Conductance calculated using the mixed FE-TB approach for three armchair MWNT models of different outer diameters, both in the undeformed and deformed configurations.

ture is present, centers of scattering are created, as in the case of bending, causing a reduction in conductivity.

For a bias voltage of 1 V, the computed overall conductance of all three undeformed tubes was the theoretical value, $G = 2G_0$. Once the deformation levels reached those shown in Figures 5 and 6, the TB code predicted a reduction in conductance that varied over the considered energy range of −0.1 to 0.3 eV (see Figure 7). The Fermi energy is again taken as a reference and shifted to zero. At the same extension, the conductance of MWNTs is found to be unchanged in the energy range where for all three undeformed tubes it was the theoretical value, $G = 2G_0$. When these energy levels are exceeded, there is a significant reduction in the conductance of the deformed tubes. Since the energy level at which conductance has the theoretical value of $2G_0$ is lower for bigger armchair MWNTs, we can conclude that for this particular load case that armchair carbon nanotubes with smaller outer diameter maintain their conductance unchanged up to higher energy levels.

CONCLUSION

In summary, a computationally effective mixed finite-element tight-binding approach has been developed which can simulate the electromechanical behavior of SWNTs and MWNTs of the dimensions used in nanoelectronic devices. The TB code is carefully designed to realize orders-of-magnitude reduction in computational time in calculating deformation-induced changes in electrical transport properties of the nanotubes. The effect of the MWNT diameter on the conductance after mechanical deformation was investigated, revealing the conductance at room temperature of MWNTs to depend strongly on the diameter, thus bigger MWNTs are more robust to changes in electrical conductivity with deformation.

Acknowledgment. This research was funded by the Ministero dell'Università e della Ricerca "Rientro dei Cervelli" funding, and in part by the AFOSR DURINT Contract No. F49620-01-1-0477. M.B.N. wishes to acknowledge the Math. Inform. and Comput. Sci. Division, Office of Adv. Sci. Comp. Res. of the U.S. Dept. of Energy under Contract No. DE-AC05-00OR22725 with UT-Battelle, the DOE-SC grant, the NSF-NIRT Grant DMR-0304299, and for partial support of this work.

REFERENCES AND NOTES

1. (a) Saito, R.; Dresselhaus, G.; Dresselhaus, M. S. *Physical Properties of Carbon Nanotubes*; Imperial College Press: London, 1998. (b) Dresselhaus, M. S.; Dresselhaus, G.; Avouris, P. *Carbon Nanotubes*; Springer: Heidelberg, 2001.
2. Bernholc, J.; Brenner, D.; Buongiorno Nardelli, M.; Meunier, V.; Roland, C. Mechanical and Electrical Properties of Nanotubes. *Annu. Rev. Mater. Res.* **2002**, *32*, 347.
3. Kong, J.; *et al.* Quantum Interference and Ballistic Transmission in Nanotube Electron Waveguides. *Phys. Rev. Lett.* **2001**, *87*, 106801.
4. Yu, M. F.; *et al.* Strength and Breaking Mechanism of Multiwalled Carbon Nanotubes under Tensile Load. *Science* **2000**, *287*, 637.
5. Tekleab, D.; Carroll, D. L.; Samsonidze, G. G.; Yakobson, B. I. Strain-Induced Electronic Property Heterogeneity of a Carbon Nanotube. *Phys. Rev. B* **2001**, *64*, 035419.
6. Frank, S.; Poncharal, P.; Wang, Z. L.; de Heer, W. A. Carbon Nanotube Quantum Resistors. *Science* **1998**, *280*, 1744.
7. Paulson, S.; *et al. In Situ* Resistance Measurements of Strained Carbon Nanotubes. *Appl. Phys. Lett.* **1999**, *75*, 2936.
8. Minot, E. D.; *et al.* Tuning Carbon Nanotube Band Gaps with Strain. *Phys. Rev. Lett.* **2003**, *90*, 156401.
9. Liu, B.; Jiang, H.; Johnson, H. T.; Huang, Y. The Influence of Mechanical Deformation on the Electrical Properties of Single Wall Carbon Nanotubes. *J. Mech. Phys. Solids* **2004**, *52*, 1.
10. Maiti, A.; Svizhenko, A.; Anantram, M. P. Electronic Transport through Carbon Nanotubes: Effects of Structural Deformation and Tube Chirality. *Phys. Rev. Lett.* **2002**, *88*, 126805.
11. Lu, J.; Wu, J.; Duan, W.; Liu, F.; Zhu, B.; Gu, B. Metal-to-Semiconductor Transition in Squashed Armchair Carbon Nanotubes. *Phys. Rev. Lett.* **2003**, *90*, 156601.
12. Farajian, A. A.; Yakobson, B. I.; Mizuseki, H.; Kawazoe, Y. Electronic Transport through Bent Carbon Nanotubes: Nanoelectromechanical Sensors and Switches. *Phys. Rev. B* **2003**, *67*, 205423.
13. Buongiorno Nardelli, M. Electronic Transport in Extended Systems: Application to Carbon Nanotubes. *Phys. Rev. B* **1999**, *60*, 7828. The computer code DOSQC ver. 1.0 is freely available at http://ermes.physics.ncsu.edu.
14. Rochefort, A.; Avouris, P.; Lesage, F.; Salahub, D. R. Electrical and Mechanical Properties of Distorted Carbon Nanotubes. *Phys. Rev. B* **1999**, *60*, 13824.
15. Yang, L.; Han, J. Electronic Structure of Deformed Carbon Nanotubes. *Phys. Rev. Lett.* **2000**, *85*, 154.
16. Sanvito, S.; Kwon, Y.; Tománek, D.; Lambert, C. J. Fractional Quantum Conductance in Carbon Nanotubes. *Phys. Rev. Lett.* **2000**, *84*, 1974.
17. Delaney, P.; Di Ventra, M.; Pantelides, S. T. Quantized Conductance of Multiwalled Carbon Nanotubes. *Appl. Phys. Lett.* **1999**, *75*, 3787.
18. Kwon, Y.; Tománek, D. Electronic and Structural Properties of Multiwall Carbon Nanotubes. *Phys. Rev. B* **1998**, *58*, R16001.
19. Choi, H. J.; Ihm, J.; Yoon, Y.; Louie, S. G. Possible Explanation for the Conductance of a Single Quantum Unit in Metallic Carbon Nanotubes. *Phys. Rev. B* **1999**, *58*, R14009.
20. Baughman, R. H.; Zakhidov, A. A.; de Heer, W. A. Carbon Nanotubes—The Route toward Applications. *Science* **2002**, *297*, 787.
21. Ke, C. H.; Espinosa, H. D.; Pugno, N. Numerical Analysis of Nanotubes Based NEMS Devices—Part II: Role of Finite Kinematics, Stretching and Charge Concentrations. *J. Appl. Mech.* **2005**, *72*, 519.
22. Ke, C. H.; Pugno, N.; Peng, B.; Espinosa, H. D. Experiments and Modeling of Carbon Nanotube NEMS Device. *J. Mech. Phys. Solids* **2005**, *53*, 1314.
23. Pugno, N.; Ke, C. H.; Espinosa, H. D. Analysis of Doubly-Clamped Nanotube Devices in the Finite Deformation Regime. *J. Appl. Mech.* **2005**, *72*, 445.
24. Pantano, A.; Parks, D. M.; Boyce, M. C. Nonlinear Structural Mechanics Based Modeling of Carbon Nanotube Deformation. *Phys. Rev. Lett.* **2003**, *91*, 145504.
25. Pantano, A.; Boyce, M. C.; Parks, D. M. Mechanics of Deformation of Single and Multiwall Carbon Nanotubes. *J. Mech. Phys. Solids* **2004**, *52*, 789.
26. Pantano, A.; Boyce, M. C.; Parks, D. M. Mechanics of Axial Compression of Single and Multi-Wall Carbon Nanotubes. *J. Eng. Mater. Technol. Trans. ASME* **2004**, *126*, 279.
27. Pantano, A.; Parks, D. M.; Boyce, M. C.; Buongiorno Nardelli, M. Mixed Finite Element-Tight-Binding Electromechanical Analysis of Carbon Nanotubes. *J. Appl. Phys.* **2004**, *92*, 6756.

28. (a) Xu, C. H.; Wang, C. Z.; Chan, C. T.; Ho, K. M. A Transferable Tight-Binding Potential for Carbon. *J. Phys.: Condens. Matter* **1992**, *4*, 6047. (b) Charlier, J. C.; Lambin, Ph.; Ebbesen, T. W. Electronic Properties of Carbon Nanotubes with Polygonized Cross Sections. *Phys. Rev. B* **1997**, *54*, R8377. (c) Porezag, D.; Frauenheim, Th.; Kohler, Th.; Seifert, G.; Kaschner, R. Construction of Tight-Binding-like Potentials on the Basis of Density-Functional Theory: Application to Carbon. *Phys. Rev. B* **1995**, *51*, 12947.
29. Meunier, V.; Buongiorno Nardelli, M.; Roland, C.; Bernholc, J. Structural and Electronic Properties of Carbon Nanotube Tapers. *Phys. Rev. B* **2001**, *64*, 195419.
30. Kuzumaki, T.; Mitsuda, Y. Dynamic Measurement of Electrical Conductivity of Carbon Nanotubes During Mechanical Deformation by Nanoprobe Manipulation in Transmission Electron Microscopy. *Appl. Phys. Lett.* **2004**, *85*, 1250.
31. Maiti, A. Mechanical Deformation in Carbon Nanotubes—Bent Tubes *vs* Tubes Pushed by Atomically Sharp Tips. *Chem. Phys. Lett.* **2000**, *331*, 21.
32. Ebbesen, T. W.; Takada, T. Topological and sp^3 Defect Structures in Nanotubes. *Carbon* **1995**, *33*, 973.